Proceedings of the 33rd European Safety and Reliability Conference (ESREL 2023)
Edited by Mário P. Brito, Terje Aven, Piero Baraldi, Marko Čepin and Enrico Zio
 Published by Research Publishing, Singapore.
doi: 10.3850/978-981-18-8071-1_P331-cd

An investigation into an alternative transition criterion of the Transitional Markov Chain Monte Carlo method for Bayesian model updating

Adolphus Lye

Singapore Nuclear Research and Safety Initiatives, National University of Singapore, Singapore.
E-mail: snrltsa@nus.edu.sg

Luca Marino

Faculty of Civil Engineering and Geoscience, Delft University of Technology, The Netherlands.
E-mail: l.marino-1@tudelft.nl

One of the advanced Monte Carlo techniques employed to perform Bayesian model updating on the epistemic model parameter(s) is the Transitional Markov Chain Monte Carlo sampler. A key characteristic in its sampling approach involves the use of "transitional" distributions to allow samples to converge iteratively from the prior to the final posterior. Hence, the selection of the transition step size becomes of critical importance. Currently, the selection criterion is such that the optimal transition step size is one that realizes a 100 % Coefficient of Variation in the statistical weights of the samples in a given iteration. The work presented here considers an alternative selection criterion on the transition step size involving the use of the Effective Sample Size as a metric. The optimal step size considered in this work is one which achieves an effective sample size equal to half the total sample size. To provide a comparative study, the standard Transitional Markov Chain Monte Carlo sampler, along with the modified Transitional Markov Chain Monte Carlo sampler imbued with the alternative selection criterion, are implemented to infer the friction force and the natural frequency of a single-storey frame structure with a metal-to-metal contact, whose dynamics is described by a non-linear differential equation. From there, the sampling performance is compared on the basis of the evolution of the tempering parameter, and the standard error of the estimates.

Keywords: Bayesian model updating, Transitional Markov Chain Monte Carlo, Parameter identification, Area metric, Non-linear dynamics, Coulomb friction.

1. Introduction

In many engineering applications, examples to which include risk analysis, reliability assessments, and structural health monitoring, an important aspect is the capability to infer model parameters under epistemic uncertainty (Lye et al. (2019, 2020)). Such uncertainties may arise from measurement "noise" when collecting data, model uncertainty, and the variability of the input model parameter due to manufacturing and material variability between the nominal identical engineering structures.

An approach to propagate and quantify the epistemic uncertainties on the inferred model parameter(s) is Bayesian model updating (Lye et al. (2019)) which will be the main focus of the work presented in the paper. One key strength to this approach is its capability to update prior knowledge while observations are made making such technique popular. To perform Bayesian model updating, advanced Monte Carlo methods are required to sample from the posterior of interest and perform numerical estimates on the inferred model parameter(s). One such method would be the Transitional Markov Chain Monte Carlo (TMCMC) sampler proposed by Ching and Chen (2007) to which details are provided in Section 2.1.

The research objectives of the paper are: 1) to consider an alternative transition criterion for the TMCMC which yields a new variant of the sampler referred to as the TMCMC-II sampler; and 2) to provide a comparison between the TMCMC and the TMCMC-II samplers in inferring the friction force and natural frequency of a single-storey frame structure with a brass-to-steel contact. Such

comparison will be done on the basis of the variability of the distribution of the posterior samples across independent sampling runs, and the number of sampling iterations elapsed.

2. Bayesian Model Updating

The Bayesian model updating technique is based upon the Bayes Theorem defined as (Beck and Katafygiotis (1998)):

$$P(\boldsymbol{\theta}|\boldsymbol{D},M) = \frac{P(\boldsymbol{\theta}|M)\cdot P(\boldsymbol{D}|\boldsymbol{\theta},M)}{P(\boldsymbol{D}|M)} \quad (1)$$

where $P(\boldsymbol{\theta}|M)$ is the prior distribution reflecting the prior knowledge on the inferred parameter(s) $\boldsymbol{\theta}$ before collecting data $\boldsymbol{D}$, $P(\boldsymbol{D}|\boldsymbol{\theta},M)$ is the likelihood function reflecting the degree of agreement between the observed data $\boldsymbol{D}$ and the prediction from model M given $\boldsymbol{\theta}$, and $P(\boldsymbol{D}|M)$ is the evidence which ensures that the posterior integrates to one.

However, due to $P(\boldsymbol{D}|M)$ being a numerical constant, it is often neglected and $P(\boldsymbol{\theta}|\boldsymbol{D},M)$ can be expressed in its un-normalised form following:

$$P(\boldsymbol{\theta}|\boldsymbol{D},M) \propto P(\boldsymbol{\theta}|M)\cdot P(\boldsymbol{D}|\boldsymbol{\theta},M) \quad (2)$$

To sample from the un-normalised $P(\boldsymbol{\theta}|\boldsymbol{D},M)$, direct Monte Carlo sampling cannot be implemented. Instead, an advanced Monte Carlo approach such as the TMCMC sampler can be adopted.

2.1. *Transitional Markov Chain Monte Carlo Sampler*

The TMCMC sampler generates samples from $P(\boldsymbol{\theta}|\boldsymbol{D},M)$ through a series of intermediate distributions known as "transitional" distributions P^j defined as (Ching and Chen (2007)):

$$P^j \propto P(\boldsymbol{\theta}|M)\cdot P(\boldsymbol{D}|\boldsymbol{\theta},M)^{\beta_j} \quad (3)$$

where $j = 0, 1, \ldots, m$ is the iteration number, and β_j is the tempering parameter such that $\beta_0 = 0 < \beta_1 < \cdots < \beta_m = 1$.

The sampling procedure undertaken by the TMCMC sampler to generate N samples from $P(\boldsymbol{\theta}|\boldsymbol{D},M)$ are as follows: At iteration $j = 0$, N samples are obtained via direct sampling from the prior $P(\boldsymbol{\theta}|M)$. Set these samples as $\boldsymbol{\theta}_i^{j+1}$, for $i = 1, \ldots, N$. At iteration $j = 1$, the algorithm proceeds to compute the normalised weights $\hat{w}_i^j$ following:

$$\hat{w}_i^j = \frac{P(\boldsymbol{D}|\boldsymbol{\theta}_i,M)^{\Delta\beta_j}}{\sum_{i=1}^N P(\boldsymbol{D}|\boldsymbol{\theta}_i,M)^{\Delta\beta_j}} \quad (4)$$

where $\Delta\beta_j = \beta_{j+1} - \beta_j$ is the transition step size. Following which, the algorithm proceeds to the Markov chain Monte Carlo step. In this step, N distinct Markov chains are generated, each initiating from $\boldsymbol{\theta}_i^j$. With probability $\hat{w}_i^j$, the sample of the i^{th} Markov chain is updated via the Metropolis-Hastings approach using a Normal proposal distribution with covariance matrix $\boldsymbol{\Sigma}^j$ computed as:

$$\boldsymbol{\Sigma}^j = \gamma^2 \cdot \sum_{i=1}^N \hat{w}_i^j \cdot \{\boldsymbol{\theta}_i^j - \overline{\boldsymbol{\theta}}^j\} \times \{\boldsymbol{\theta}_i^j - \overline{\boldsymbol{\theta}}^j\}^T \quad (5)$$

where γ is the scaling parameter set at 0.2 (Ching and Chen (2007)), and $\overline{\boldsymbol{\theta}}^j = \frac{1}{N}\sum_{i=1}^N \boldsymbol{\theta}_i^j$ is the sample mean. This method of updating the samples is repeated N times which implies that the Markov chain with higher $\hat{w}_i^j$ would have longer chains assembled. The resulting set of updated samples are then set as $\boldsymbol{\theta}_i^{j+1}$ and the algorithm proceeds to iteration $j = j + 1$. This process is repeated until the last iteration $j = m$.

An important aspect of the TMCMC sampler is the selection of an optimal $\Delta\beta_j$. Such value of $\Delta\beta_j$ should neither be too small such that the sampling procedure requires a relatively larger number of iterations, nor too large such that the transition between P^j and P^{j+1} no longer becomes gradual. As proposed by Ching and Chen (2007), the optimal value of $\Delta\beta_j$ at any given j is one that ensures that the Coefficient of Variation of $P(\boldsymbol{D}|\boldsymbol{\theta},M)^{\Delta\beta_j}$ is $100\ \%$. This can be done numerically by solving the following optimisation problem (Ching and Chen (2007)):

$$\beta_{j+1} = \text{argmin}_{\beta_{j+1}} \left\{ \left| \frac{\sigma(P(\boldsymbol{D}|\boldsymbol{\theta}_i^j,M)^{\Delta\beta_j})}{\mu(P(\boldsymbol{D}|\boldsymbol{\theta}_i^j,M)^{\Delta\beta_j})} - 1 \right| \right\} \quad (6)$$

where $\sigma(\bullet)$ and $\mu(\bullet)$ are the standard deviation and mean operators respectively.

2.2. *Proposed Transition Criterion*

The paper presents an alternative transition criterion involving the use of a metric known as the Effective Sample Size N_{eff} which serves as an indicator of sample degeneracy. The metric N_{eff} is computed at every iteration j following (Liu and Chen (1998)):

$$N_{eff} = \frac{1}{\sum_{i=1}^{N} \left(\hat{w}_i^j\right)^2} \tag{7}$$

where $\hat{w}_i^j$ is computed via Eq. (4). As a reference, Liu and Chen (1998) proposed a threshold value of $N_{eff} = \frac{N}{2}$ below which, it indicates the presence of sample degeneracy. Such approach of highlighting sample degeneracy and providing a criterion for resampling has been implemented within the Sequential Monte Carlo samplers by Moral et al. (2006). With reference to Eq. (4), the formula for N_{eff} can be re-expressed as:

$$N_{eff}(\Delta\beta_j) = \frac{\left(\sum_{i=1}^{N} P(\boldsymbol{D}|\boldsymbol{\theta}_i^j, M)^{\Delta\beta_j}\right)^2}{\sum_{i=1}^{N} \left(P(\boldsymbol{D}|\boldsymbol{\theta}_i^j, M)^{\Delta\beta_j}\right)^2} \tag{8}$$

From there, the following optimisation problem is presented and solved numerically:

$$\beta_{j+1} = \text{argmin}_{\beta_{j+1}} \left\{ \left| N_{eff}(\Delta\beta_j) - \frac{N}{2} \right| \right\} \tag{9}$$

For the purpose of distinction from the original TMCMC sampler, the resulting sampler adopting this transition criterion will be referred to as the TMCMC-II sampler. To provide a comparison between the sampling performances of the TMCMC and the TMCMC-II samplers, the samplers will be implemented to infer key parameters of a nonlinear dynamical engineering structure to which details are presented in Section 3.

3. Benchmark Application Problem

The benchmark application problem involves the inference of natural frequency and friction force in a base-excited single-storey frame with a brass-to-steel contact from its measured bottom-plate and top-plate displacements. This experimental setup has already been extensively investigated in Marino and Cicirello (2020); Lye et al. (2023),

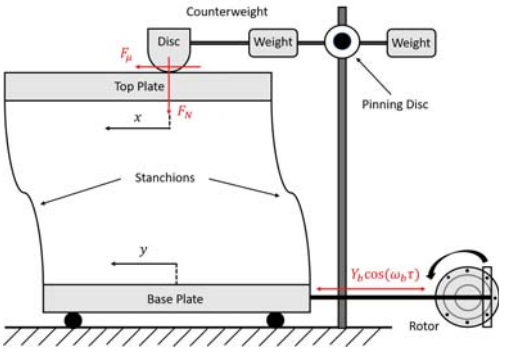

Fig. 1. Schematic diagram of the single-storey frame experimental setup. Image adopted from Lye et al. (2023).

where a detailed description of test rig and procedure is available. A schematic diagram of the structure is provided in Figure 1.

3.1. *Physics-based Model*

As demonstrated by Marino and Cicirello (2020), the single-storey frame can be modelled as a Single-Degree-of-Freedom (SDoF) mass-spring system with a friction contact between the mass and an external wall, and Coulomb's law can be used as a friction model. The physics-based model of this structure is therefore governed by the following non-linear differential equation:

$$r^2 \cdot \frac{d^2\tilde{x}}{d{\tau_b}^2} + \tilde{x} + \varphi \cdot \text{sgn}\left(\frac{d\tilde{x}}{d\tau_b}\right) = \cos(\tau_b) \tag{10}$$

where $\tilde{x}$ is the dimensionless displacement of the top plate, r is the dimensionless frequency ratio, φ is the dimensionless friction force, τ_b is the dimensionless time parameter, and $\text{sgn}(\bullet)$ is the sign function. The dimensionless parameters are mathematically defined as follows:

$$\tilde{x} = \frac{x}{Y_b} \tag{11}$$

$$r = \frac{\omega_b}{\omega_n} \tag{12}$$

$$\varphi = \frac{F_\mu}{k \cdot Y_b} \tag{13}$$

$$\tau_b = \omega_b \cdot t \tag{14}$$

where Y_b is the amplitude of the base excitation, k is the stiffness of the SDoF model, $k \cdot Y_b = 2.50$ N is the driving force, ω_b is the driving frequency, $\omega_n = 3.086\ Hz$ is the natural frequency of the system, and $F_\mu = 1.086\ N$ is the amplitude of the Coulomb friction force generated in the contact.

Under the assumption of steady-state continuous motion, the analytical solution to Eq.(10) can be written in the half-period $[0, \pi)$ included between a maximum and the subsequent minimum of $\tilde{x}(\tau_b)$ as (Den-Hartog (1930)):

$$\tilde{x}(\tau_b) = \tilde{x}_0 \cdot \cos(\tau_b) + \varphi \cdot U \cdot \sin(\tau_b) + \varphi \cdot \left[1 - \cos\left(\frac{\tau_b}{r}\right) - U \cdot r \cdot \sin\left(\frac{\tau_b}{r}\right)\right] \quad (15)$$

and as $-\tilde{x}(\tau_b - \pi)$ in the subsequent half-period $[\pi, 2\pi)$. In the above equation, U is the damping function defined as:

$$U = \frac{\sin(\pi/r)}{r \cdot [1 + \cos(\pi/r)]} \quad (16)$$

while $\tilde{x}_0$ is the dimensionless response amplitude defined as:

$$\tilde{x}_0 = \sqrt{\left(\frac{1}{1 - r^2}\right)^2 - (\varphi \cdot U)^2} \quad (17)$$

Detailed explanation behind their derivations can be found in Marino et al. (2019).

3.2. *Generating the Numerical Data*

The numerical data of interest, for a fixed value of the friction force F_μ, are the frequency ratio r and the corresponding phase angle ϕ. The model relating F_μ and r to ϕ is denoted as M_ϕ and its implementation is done in the following steps:

(1) The model computes φ using Eq. (13);
(2) The algorithm computes the boundary between continuous and stick-slip regimes following (Den-Hartog (1930)):

$$\varphi_{lim} = \sqrt{\frac{1}{\left(U^2 + \frac{1}{r^4}\right) \cdot (1 - r^2)^2}} \quad (18)$$

(3) If $\varphi > \varphi_{lim}$, the assumption of continuous motion is not satisfied and, since the current analysis is limited to continuous responses, the model assigns a NaN (i.e. Not a Number) value for ϕ before terminating the procedure. Otherwise, the algorithm proceeds to the next step;
(4) The algorithm computes $\tilde{x}(\tau_b)$ from Eq. (15) and the numerical forcing function $\tilde{y}(\tau_b)$:

$$\tilde{y}(\tau_b) = \cos(\tau_b + \eta) \quad (19)$$

in the time interval $[0, 2\pi)$, being:

$$\eta = \text{atan2}\left[-\varphi \cdot U \cdot (1 - r^2),\ \tilde{x}_0 \cdot (1 - r^2)\right] \quad (20)$$

(5) The dimensionless frequency spectra $\tilde{x}_{FFT}(\tilde{f})$ and $\tilde{y}_{FFT}(\tilde{f})$ are obtained using the Fast-Fourier Transformation on $\tilde{x}(\tau_b)$ and $\tilde{y}(\tau_b)$ respectively;
(6) Setting $\tilde{f} = 1$ (i.e., the dimensionless driving frequency), the resulting ϕ is computed following (Marino and Cicirello (2020)):

$$\phi = \arg\{\tilde{x}_{FFT}(\tilde{f} = 1)\} - \arg\{\tilde{y}_{FFT}(\tilde{f} = 1)\} \quad (21)$$

A summary to the above procedure is provided as a pseudo-algorithm as shown in Algorithm 1. In the event $M_\phi = \text{NaN}$, the likelihood function $P(\boldsymbol{D}^s|\boldsymbol{\theta}, M_\phi, M_r)$ returns a 0.

In total, 10 different sets of data $\boldsymbol{D} = \{r_{nom}, r, \omega_b, \phi\}$ are obtained numerically. To simulate measurement "noise", the numerical data for r and ϕ are obtained following:

$$r = r_{nom} + \epsilon_r; \quad \text{where } \epsilon_r \sim N(0, \sigma_r) \quad (22)$$

where $\sigma_r = 0.01$, and r_{nom} is the nominal frequency ratio used for data collection, from which ω_b is computed from r using Eq. (12), and

$$\phi = M_\phi + \epsilon_\phi; \quad \text{where } \epsilon_\phi \sim N(0, \sigma_\phi) \quad (23)$$

where $\sigma_\phi = 2^o$. The resulting data values for $\boldsymbol{D}$ are presented in Table 1 and are illustrated as a graphical plot in Figure 2.

3.3. *Bayesian Model Updating Set-up*

The Bayesian model updating procedure is implemented to infer $\boldsymbol{\theta} = \{F_\mu, \omega_n\}$. It needs to be noted that the inferred parameters defined by $\boldsymbol{\theta}$ are assumed to be time-invariant.

Assuming independence between the distinct sets of data and the inferred parameters, the likeli-

Algorithm 1 Pseudo-algorithm of model M_ϕ

procedure (Compute ϕ from F_μ and r)
  Compute φ with F_μ using Eq. (13)
  Compute φ_{lim} with r using Eq. (18)
  if $\varphi > \varphi_{lim}$ **then** ▷ Continuous motion condition not satisfied
    Set $\phi = \text{NaN}$
  else
    Compute $\tilde{x}(\tau_b)$ using Eq. (15)
    Compute $\tilde{y}(\tau_b)$ using Eq. (19)
    Execute FFT on $\tilde{x}(\tau_b)$ to yield $\tilde{x}_{FFT}(\tilde{f})$
    Execute FFT on $\tilde{y}(\tau_b)$ to yield $\tilde{y}_{FFT}(\tilde{f})$
    Set $\tilde{f} = 1$
    Compute ϕ using Eq. (21)
  end if
end procedure

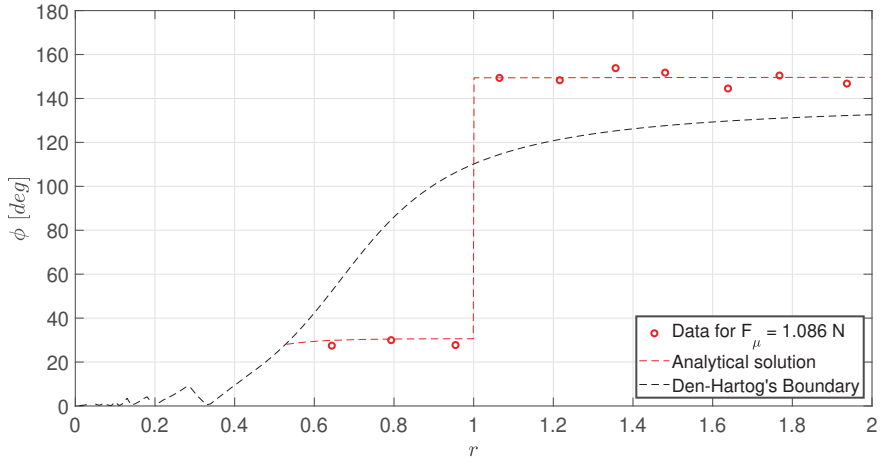

Fig. 2. Plot of the data of phase angle ϕ $[deg]$ against the dimensionless frequency ratio r.

hood function is defined as:

$$P(\boldsymbol{D}|\boldsymbol{\theta}, M) = \prod_{q=1}^{10} \frac{1}{2\pi \cdot \sigma_r \cdot \sigma_\phi} \times \exp\left[-\frac{(r^q_{nom} - M_r(\omega^q_b, \omega_n))^2}{2 \cdot {\sigma_r}^2} - \right] \times \exp\left[\frac{(\phi^q - M_\phi(r^q, F_\mu))^2}{2 \cdot {\sigma_\phi}^2} \right] \quad (24)$$

where M_r is the model used to predict r as defined by Eq. (12), and $M = \{M_\phi, M_r\}$. Here, σ_r and σ_ϕ are set as uncertain parameters.

For the inferred parameters, each of them are assigned a Uniform prior with bounds defined in Table 2. A Uniform prior is chosen to simulate the lack of prior knowledge on the true value of the epistemic parameters and that only the bounds are known.

For both the TMCMC and the TMCMC-II samplers, a total of $N = 1000$ samples are obtained from the resulting posterior $P(\boldsymbol{\theta}|\boldsymbol{D}, M)$.

Table 1. The numerical data generated for $\boldsymbol{D}$.

S/N	r_{nom}	r	ω_b (Hz)	ϕ (deg)
1	0.643	0.644	1.987	27.466
2	0.786	0.793	2.447	29.968
3	0.929	0.954	2.945	27.739
4	1.071	1.065	3.286	149.366
5	1.214	1.216	3.753	148.301
6	1.357	1.356	4.186	153.816
7	1.500	1.481	4.569	151.774
8	1.643	1.639	5.056	144.536
9	1.786	1.768	5.455	149.090
10	1.929	1.937	5.978	149.947

Table 2. Uniform prior bounds for the respective inferred parameters.

Parameter	Bounds	Units
F_μ	$[0.01, 10]$	N
ω_n	$[0.01, 10]$	Hz
σ_ϕ	$[0.001, 10]$	deg
σ_r	$[0.001, 1]$	$-$

To account for the variability in the posterior samples generated and their distributions due to the stochastic nature of the sampling procedure by the samplers, the sampling procedure is repeated 50 times. From which, the performance of the respective samplers are compared on the basis of: 1) variability of the resulting distribution of the posterior samples; and 2) the statistics on the total number of iterations required for the sampling procedure.

4. Results and Discussions

From the resulting 50 sampling runs, a P-box is constructed from the Empirical CDF (ECDF) of the posterior samples (Ferson et al. (2003)). The P-boxes are presented graphically for F_μ and ω_n as shown in Figure 3. As seen in the Figure, the P-boxes for F_μ and ω_n obtained by the respective samplers both encompass the corresponding true values of the inferred parameters. However, it is noteworthy that the area of the P-box obtained for both inferred parameters are significantly larger for the case of the TMCMC-II sampler compared to that obtained by the TMCMC sampler. To support such observation, the area metric A is computed for the respective P-boxes following (De-Angelis and Gray (2021)):

$$A = \int_{-\infty}^{\infty} |F_L(x) - F_U(x)| \cdot dx \qquad (25)$$

where $F_L(\bullet)$ is the lower bound ECDF of the P-box, and $F_U(\bullet)$ is the upper bound ECDF of the P-box. The numerical results of A are presented in Table 3 for the corresponding P-boxes by the respective samplers, and such result is supplemented by a bar chart illustrated in Figure 4.

Table 3. Numerical results of the area metric for the corresponding P-boxes obtained by the respective samplers.

Sampler	Area of P-box	
	F_μ (N)	ω_n (Hz)
TMCMC	8.151×10^{-2}	8.878×10^{-3}
TMCMC-II	1.714×10^{-1}	8.915×10^{-3}

It is noteworthy from Table 3 and Figure 4 that the area of the P-box for F_μ obtained by the TMCMC-II sampler is nearly twice as large compared to that obtained by the TMCMC sampler. This indicates a larger degree of variability in the posterior samples of F_μ obtained by the TMCMC-II sampler. Such observation highlights a poor convergence rate of the samples to the true posterior distribution, indicating a relatively poor mixing performance by the sampler.

The resulting statistics of the total number of sampling iterations elapsed by the TMCMC and the TMCMC-II samplers across the 50 sampling runs are presented numerically in Table 4 and graphically in Figure 4. Based on the statistics, while most the sampling runs by both the TMCMC and the TMCMC-II samplers require 11 iterations, it is noteworthy that the maximum number of sampling iterations required by the TMCMC-II sampler to sample from the posterior distribution is 11 whilst that of the TMCMC sampler is 10. In fact, 9 of such sampling runs

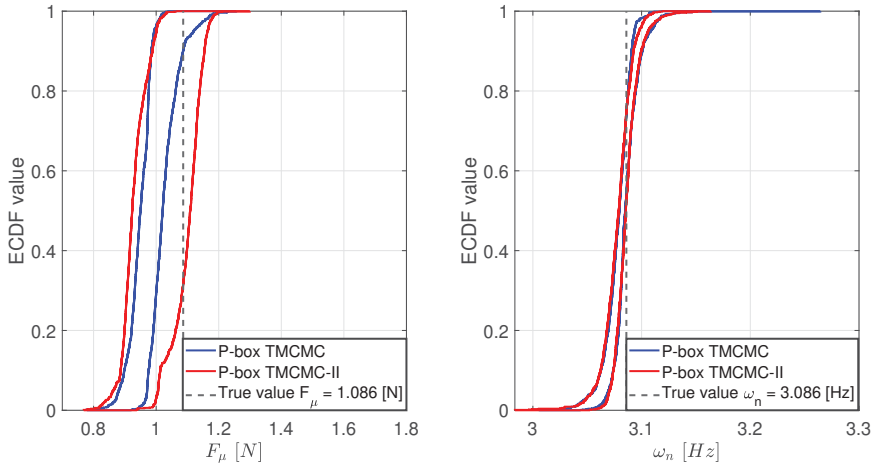

Fig. 3. Resulting P-boxes of the estimates for the friction force F_μ and natural frequency ω_n obtained by the TMCMC and the TMCMC-II samplers.

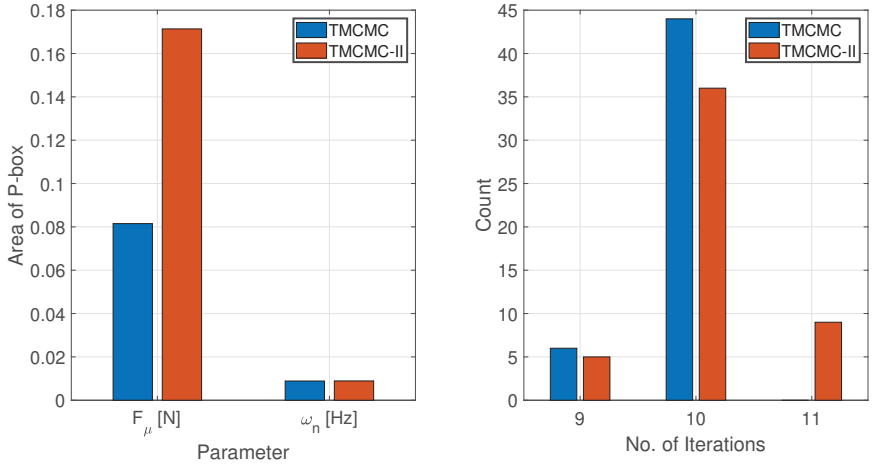

Fig. 4. Bar charts illustrating the statistics for the area of the P-box obtained for the respective inferred parameters (left), and the statistics of the total number of sampling iterations elapsed (right) by the TMCMC and the TMCMC-II samplers.

by the TMCMC-II require 11 sampling iterations in sampling from the posterior distribution which constitutes 18 % of the total number of sampling runs. This provides additional evidence of the relatively poor mixing performance by the TMCMC-II sampler compared to the TMCMC sampler.

5. Conclusion

The paper has presented an alternative transition criterion for the Transitional Markov Chain Monte Carlo sampler. It involves the use of the Effective Sample Size as a metric to determine the transition step size such that the transition occurs upon the

Table 4. Numerical statistics of the total number of sampling iterations elapsed by the respective samplers.

No. of Iterations	Sampler	
	TMCMC	TMCMC-II
9	6	5
10	44	36
11	0	9

Effective Sample Size reaching half of the total sample size.

To study the effectiveness of such transition criterion, the modified variant of the sampler is implemented alongside the traditional variant to infer key parameters of an experimental test rig modelled as a Single-Degree-of-Freedom system subjected to Coulomb friction. The comparison between the samplers are done on the basis of the variability of the posterior sample distribution and the number of sampling iterations required.

Results showed a greater degree of variability in the distribution of the posterior samples as well as significant sampling runs requiring a relatively higher number of sampling iterations by the modified Transitional Markov Chain Monte Carlo sampler compared to the traditional variant. This indicates a relatively poor mixing performance by the former. Further investigations are required to provide non-empirical reasoning(s) behind such observation.

To allow for a better understanding of the study presented, MATLAB codes to the sampling algorithms, model, and the benchmark application problem are made accessible on GitHub via: `https://github.com/Adolphus8/Bayesian-Model-Updating-Tutorials.git`. Experimental data are also available on GitHub via: `https://github.com/l-marino/singlestorey-friction`.

Acknowledgement

The lead author would like to acknowledge the support of the Singapore Nuclear Research and Safety Initiatives in this endeavour.

References

Beck, J. L. and L. S. Katafygiotis (1998). Updating Models and Their Uncertainties I: Bayesian Statistical Framework. *Journal of Engineering Mechanics 124*, 455—-461.

Ching, J. and Y. Chen (2007). Transitional markov chain monte carlo method for bayesian model updating, model class selection, and model averaging. *Journal of Engineering Mechanics 133*, 816—-832.

De-Angelis, M. and A. Gray (2021). Why the 1-Wasserstein distance is the area between the two marginal CDFs. *arXiv*.

Den-Hartog, J. P. (1930). Forced vibrations with combined viscous and Coulomb damping. *The London, Edinburgh, and Dublin Philosophical Magazine and Journal of Science 9*, 801–817.

Ferson, S., V. Kreinovich, L. Ginzburg, K. Sentz, and D. S. Myers (2003). Constructing probability boxes and Dempster-Shafer structures. *Sandia National Laboratories*.

Liu, J. S. and R. Chen (1998). Sequential Monte Carlo Methods for Dynamic Systems. *Journal of the American Statistical Association 93*, 1032–1044.

Lye, A., A. Cicirello, and E. Patelli (2019). A Review of Stochastic Sampling Methods for Bayesian Inference Problems. *In Proceedings of the 29th European Safety and Reliability Conference 1*, 1866–1873.

Lye, A., A. Cicirello, and E. Patelli (2020). Bayesian Model Updating of Reliability Parameters using Transitional Markov Chain Monte Carlo with Slice Sampling. *In Proceedings of the 30th European Safety and Reliability Conference and 15th Probabilistic Safety Assessment and Management Conference 1*, 2734–2741.

Lye, A., L. Marino, A. Cicirello, and E. Patelli (2023). Sequential Ensemble Monte Carlo sampler for Online Bayesian inference of Time-varying Model parameters in Engineering Applications. *ASME Journal of Risk and Uncertainty Part B 9*, 031202.

Marino, L. and A. Cicirello (2020). Experimental investigation of a single-degree-of-freedom system with Coulomb friction. *Nonlinear Dynamics 99*, 1781–1799.

Marino, L., A. Cicirello, and D. A. Hills (2019). Displacement transmissibility of a Coulomb friction oscillator subject to joined base-wall motion. *Nonlinear Dynamics 98*, 2595—2612.

Moral, P. D., A. Doucet, and A. Jasra (2006). Sequential Monte Carlo Samplers. *Journal of the Royal Statistical Society. Series B (Statistical Methodology) 68*, 411–436.